International Journal of Heat and Mass Transfer 52 (2009) 3606–3612

Contents lists available at ScienceDirect

International Journal of Heat and Mass Transfer

journal homepage: www.elsevier.com/locate/ijhmt

Heat transfer to a silicon carbide/water nanofluid

Wenhua Yu [a,*], David M. France [b], David S. Smith [a], Dileep Singh [c], Elena V. Timofeeva [a], Jules L. Routbort [a]

[a] Energy Systems Division, Argonne National Laboratory, 9700 South Cass Avenue, Argonne, IL 60439, USA
[b] Department of Mechanical and Industrial Engineering, University of Illinois at Chicago, 842 West Taylor Street (m/c 251), Chicago, IL 60607, USA
[c] Nuclear Engineering Division, Argonne National Laboratory, 9700 South Cass Avenue, Argonne, IL 60439, USA

ARTICLE INFO

Article history:
Received 10 December 2008
Received in revised form 12 February 2009
Accepted 12 February 2009
Available online 16 April 2009

Keywords:
Nanofluids
Heat transfer
Turbulent flow
Silicon carbide

ABSTRACT

Heat transfer experiments were performed with a water-based nanofluid containing 170-nm silicon carbide particles at a 3.7% volume concentration and having potential commercial viability. Heat transfer coefficients for the nanofluid are presented for Reynolds numbers ranging from 3300 to 13,000 and are compared to the base fluid water on the bases of constant Reynolds number, constant velocity, and constant pumping power. Results were also compared to predictions from standard liquid correlations and a recently altered nanofluid correlation. The slip mechanisms of Brownian diffusion and thermophoresis postulated in the altered correlation were investigated in a series of heating and cooling experiments.

Published by Elsevier Ltd.

1. Introduction

A nanofluid generally refers to a liquid mixture with a small concentration of nanometer-sized solid particles in suspension. Some combinations of nanoparticles and liquids have been shown to substantially increase the thermal conductivity of the nanofluid over the base liquid. See, for example, review articles [1–4]. The proposed applications of nanofluids have generally been in the heat transfer area where a small concentration of particles often produces an-order-of-magnitude-larger heat transfer enhancement [1–4].

Nanofluid heat transfer is a relatively new field being little more than a decade old. During that time, research groups worldwide have focused on determining the levels of thermal enhancement of a variety of nanofluids. In these investigations, the emphasis was usually on the magnitude of the thermal phenomena and not on the viability of the fluids for commercial applications. In the early stages of investigation, it was more important to establish the enhancement potential of nanofluids before considering applications. There were a number of review papers during that period, for example, references [1–4] with commentary [5] and a recent book [6]. These articles include discussions on the preparation of nanofluids as well as their thermal and transport properties. The thermal conductivity in particular has received considerable attention by researchers. It is easier to measure than the heat transfer coefficient and has been used as an indicator of nanofluid heat transfer enhancement.

A recent review article [7] concentrated on both the thermal conductivity and heat transfer rates of nanofluids as presented in the literature through 2006. Eight important parameters were reviewed and assessed individually (1) particle volume concentration, (2) particle material, (3) particle size, (4) particle shape, (5) base fluid, (6) temperature, (7) additive, and (8) pH. Experimental results from multiple research groups were used together when assessing results and determining repeatable trends. Some research groups [8,9] have found that the heat transfer enhancement was close to predictions from standard liquid heat transfer correlations using the nanofluid properties. In another study [10], the enhancement was up to 40% above such predictions. This phenomenon will be discussed subsequently with respect to the SiC/water nanofluid data of this study coupled with heat transfer enhancement mechanisms. However, Nusselt number enhancement of 40% is attractive to many applications if the nanofluid is commercially viable – no matter if the enhancement is predictable with existing liquid correlations or if it requires predictive correlations specific to nanofluids.

Today the nanofluid field has developed to the point where it is appropriate to look to the next level, i.e., nanofluids that show substantial heat transfer enhancement over their base fluids and are candidates for use in industrial/commercial systems. At a minimum, nanofluids acceptable for widespread industrial use would be stable suspensions with little or no particle settling, available in large quantities at affordable cost, environmentally neutral, and non-toxic. In addition, such applications would generally require that there be little change in particle agglomeration over time and that the nanofluid not be susceptible to adverse surface adhesion. In a related study [11], the properties and characteristics

* Corresponding author. Tel.: +1 630 252 7361; fax: +1 630 252 5568.
E-mail address: wyu@anl.gov (W. Yu).

0017-9310/$ - see front matter Published by Elsevier Ltd.
doi:10.1016/j.ijheatmasstransfer.2009.02.036

Nomenclature

C_p	specific heat
D	test section outside diameter
d	test section inside diameter
h	heat transfer coefficient
k	thermal conductivity
Mo	Mouromtseff number
Nu	Nusselt number
Pr	Prandtl number
q'	heat per unit length
q''	heat flux
Re	Reynolds number
T	temperature
v_p	particle volume concentration
x	axial distance

Greek symbols

μ	viscosity
ρ	density

Subscripts

c	cooling water
e	nanofluid
in	inlet
m	base fluid matrix
out	outlet
p	particle
w	test section wall

of a potentially viable SiC/water nanofluid for commercial applications were verified and quantified more extensively than found elsewhere in the literature with positive results, e.g., no particle settling, large quantity availability, environmentally neutral, and little agglomeration. A carbide material was chosen for the nanoparticles for several reasons including the absence of oxidation, and SiC in particular was chosen for its high thermal conductivity. In the present study, the first experimental heat transfer results are reported for a SiC/water nanofluid. The conditions are for the turbulent flow of a 3.7 vol.% SiC/water nanofluid, and results are compared to the base fluid water as well as to heat transfer predictions from accepted correlations for liquids. Nanofluids are also compared on the basis of the combined effects of heat transfer enhancement and pumping power increase. Heat transfer enhancement mechanisms in nanofluids are discussed, and results are presented from experiments conducted to study the slip mechanisms of Brownian diffusion and thermophoresis.

2. Nanofluid characterization

Most studies of thermal phenomena in nanofluids have failed to make detailed characterizations of the fluids. It is known that particle agglomeration occurs in many nanofluids so that the nominal particle size in a powder is often not the size in the suspension. In fact, particle size distributions exist in the nanofluids but are seldom measured. As a result, literature data reported based on nominal particle size may in fact have involved significantly different average particle sizes and distributions in suspensions.

The SiC/water nanofluid of this study was characterized [11] in detail including very important information about particle size distribution in suspension. The average size of 170 nm was measured by both dynamic light scattering (Brookhaven Instruments Corp., Holtsville, NY) and small angle X-ray scattering (beamline 15-ID-D, Advanced Photon Source, Argonne National Laboratory, Argonne, IL). The thermal conductivity of the nanofluid was measured by a transient hot wire probe over a temperature range of 25–70 °C and was found to be consistently 22% higher than that of water. A viscometer (Brookfield viscometer model DV-II+Pro, Middleboro, MA) was used to measure the viscosity of the nanofluid. The measured nanofluid viscosity varied from 1.8 to 2.0 times the viscosity of water depending on temperature and fit well to the empirical equation

$$\mu = 0.00496(e^{1736.6/T}) \tag{1}$$

where T is the temperature in the unit of Kelvin and μ is the viscosity in the unit of centipoise.

These results show that the SiC/water nanofluid is well behaved, the thermal conductivity enhancement is reasonably high, and the viscosity increase is relatively low. Settling and agglomeration do not occur, and all of these conditions contribute to the potential commercial viability of the fluid.

In order to determine nanofluid heat transfer coefficients from experimental measurements or from correlations based on such experiments, nanofluid density and heat capacity are usually required. In the present study, the effective density and specific heat were calculated based on the physical principle of the mixture rule as

$$\rho_e = (1 - v_p)\rho_m + v_p\rho_p \tag{2}$$

$$C_{pe} = \frac{(1 - v_p)(\rho C_p)_m + v_p(\rho C_p)_p}{\rho_e} = \frac{(1 - v_p)(\rho C_p)_m + v_p(\rho C_p)_p}{(1 - v_p)\rho_m + v_p\rho_p} \tag{3}$$

This is the standard equation for nanofluid specific heat, and the effective specific heat determined through energy balances during the experiments in this study was found to be within 1% of the calculation.

3. Test facility

The nanofluid heat transfer test facility at Argonne National Laboratory was designed and fabricated to study the characteristics of single-phase and two-phase heat transfer under conditions of small channel and low mass fluxes for nanofluids. As shown in Fig. 1, the test facility is a closed-loop system with major components consisting of a pump with variable speed drive, preheater, horizontal tube test section, heat exchanger (cooler), and flowmeter. For the SiC/water nanofluid, the maximum system operating pressure and temperature were 273 kPa and 100 °C, respectively, and the system flow rate was in the range of 350–1700 ml/min. The preheater provides a means to set the inlet temperature to the test section at desired levels. The test section itself is a type 316 stainless steel circular tube with dimensions of 2.27-mm inside diameter, 4.76-mm outside diameter, and 0.58-m heated length. The preheater and test section are individually resistance-heated with controllable direct current power supplies and are electrically isolated from the remainder of the facility with short sections of high-pressure hose, designated ISO in Fig. 1. As a safety precaution, both the preheater and test section are provided with high-temperature-limit interlocks to prevent them from being overheated. Thermocouples are used to measure wall and fluid temperatures along the test section heated length for calculating heat transfer coefficients. The pressure at the test section inlet and pressure drop across the test section are also measured by using electronic pressure transducers. Pressure transducers,

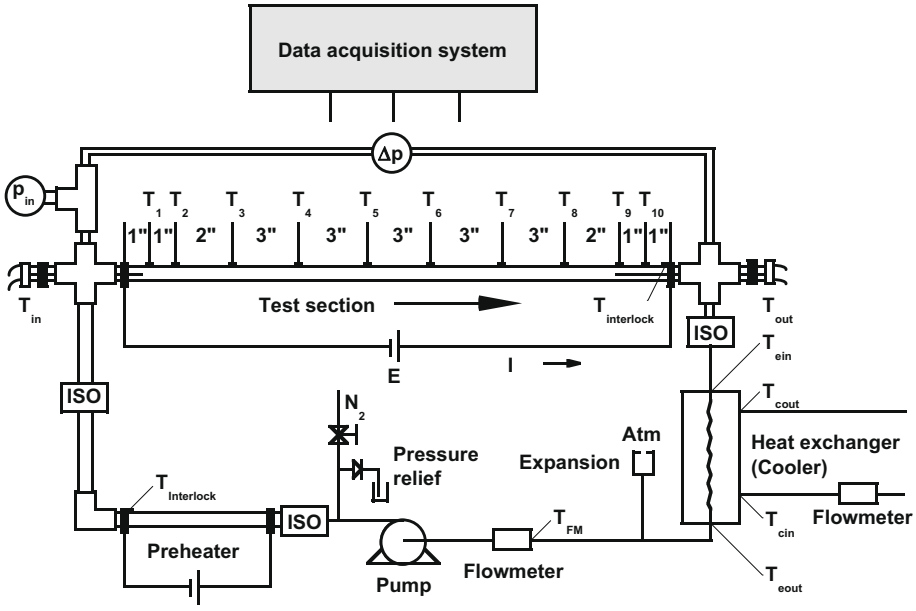

Fig. 1. Schematic diagram of test facility.

flowmeter, and thermocouples were calibrated against standards traceable to the National Institute of Standards and Technology. The estimated uncertainty in the measurements of pressures, flowrate, and temperatures are ±3%, ±1%, and ±0.2 °C, respectively.

A data acquisition system consisting of a computer and a Hewlett–Packard multiplexer was assembled to record outputs from all sensors. A data acquisition program, which includes all calibration equations and conversions to desired engineering units, was written. The data acquisition system provides an on-screen display of signals from all sensors and graphs of representative in-stream and wall temperature measurements for steady-state monitoring. When desired test conditions are reached, the data acquisition system records multiple readings of temperatures, power input, fluid flow rate, and pressures for subsequent data reduction.

Although the test section was well thermally insulated from the atmosphere and the test section heat loss was small (less than 1%) during heat transfer tests, the heat loss was incorporated into the data reduction procedure for improving accuracy.

4. Heat transfer data reduction

A series of experiments was carried out to investigate the characteristics of forced convective heat transfer under conditions of horizontal turbulent flow, small channel, and low mass flux for a 3.7 vol.% SiC/water nanofluid. Tests were performed at atmospheric pressure at the pump suction. At steady-state conditions, all sensor outputs were read 30 times by the data acquisition system and then averaged together for future processing. These data included 10 test section outside wall temperatures (T_1–T_{10}), test section inlet and outlet fluid temperatures (T_{in} and T_{out}), test section inlet fluid pressure (p_{in}), overall pressure drop across the test section (Δp), current through the test section (I), voltage drop across the test section (E), test fluid flow rate, temperature at the pump (T_{FM}), heat exchanger (cooler) inlet and outlet temperatures of the nanofluid and cooling water (T_{ein}, T_{eout}, T_{cin}, and T_{cout}), cooling water flow rate, and ambient temperature.

The local convective heat transfer coefficient at position x along the length of the test section is defined as

$$h(x) = \frac{q''(x)}{T_{win}(x) - T_e(x)} \tag{4}$$

In Eq. (4), the local surface heat flux $q''(x)$ was determined from the measured voltage and current (corrected for losses) of the test section heater and the local electrical resistivity of the tube as a function of temperature along the test section. The inner wall surface temperature of the test section $T_{win}(x)$ was determined from a radial heat conduction calculation by using the measured outer surface temperature $T_{wout}(x)$ and the local heat generated in the test section wall per unit length $q'(x)$

$$T_{win}(x) = T_{wout}(x) + \frac{q'(x)}{4\pi k_w(x)} \frac{1 + \ln(d/D)^2 - (d/D)^2}{1 - (d/D)^2} \tag{5}$$

The local nanofluid temperature $T_e(x)$ was calculated, from a linear relation between test section inlet and outlet temperatures, at the same location where the wall temperature $T_{wout}(x)$ was measured. The nanofluid temperatures could also be obtained from a heat balance using the measured inlet nanofluid temperature and the test section power. These two methods were in good agreement with each other.

This experimental technique provided local heat transfer coefficient data at multiple positions along the test section during any experiment. This approach has increased accuracy compared to other techniques found in the literature where average results were reported over the entire test section length [7–9]. Depending on how the tests were conducted, there could be significant changes in fluid properties, Reynolds number, etc. along that length, which would decrease the accuracy of the averaging technique.

The uncertainties in the nanofluid convective heat transfer coefficients, determined from the parameters described, were <5% in all cases. The uncertainty was calculated by the method of sequential perturbation, as described by Moffat [12]. This method is for single-sample data in which uncertainties in each independent variable, used to calculate the nanofluid convective heat transfer coefficient, were estimated based on their individual calibrations.

5. Base fluid heat transfer tests

Heat transfer tests were performed on the base fluid water to provide a baseline for comparison to nanofluid data, and they also served as control tests for the test facility. Fig. 2 shows that the

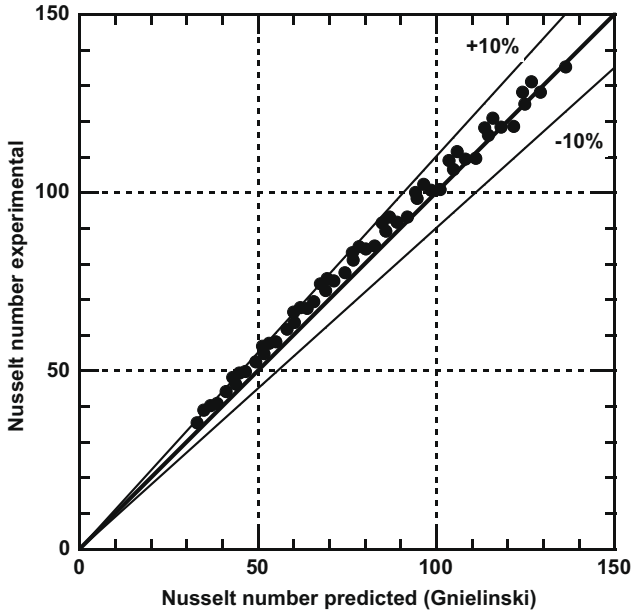

Fig. 2. Nusselt number comparison for water.

experimental Nusselt numbers for water are in good agreement with the predicted values from Gneilinski equation [13] with most of the differences less than 10%. This excellent agreement serves as an overall verification of the facility, sensors, data acquisition, and data reduction procedures.

6. Nanofluid heat transfer results and discussions

6.1. Nusselt numbers

A series of experiments of forced convective heat transfer for a 3.7 vol.% SiC/water nanofluid was carried out with the following experimental parameters: Reynolds number of 3300–13,000, Prandtl number of 4.6–7.1, and local nanofluid temperature for heat transfer coefficient determination of 34–57 °C. The temperature difference between the inner test section wall and the fluid, a key parameter in minimizing experimental errors, was above 10 °C in all cases. Results are shown in Fig. 3 compared to the water data. The Nusselt numbers are plotted against the parameter $Re^{0.8}$ $Pr^{0.4}$ taken from the Dittus–Boelter correlation [14]. Use of this parameter incorporates temperature effects on fluid properties. The nanofluid data of Fig. 3 are seen to be above the water data in all cases showing an enhancement over the base fluid taken at equal values of the parameter $Re^{0.8}$ $Pr^{0.4}$.

6.2. Heat transfer enhancement above base fluid

The nanofluid heat transfer enhancement over its base fluid water is shown in detail in Fig. 4. Here the heat transfer enhancement, the ratio of the experimental nanofluid heat transfer coefficient to the predicted water heat transfer coefficient from the Gneilinski correlation, is plotted. Compared on the basis of Reynolds number (the most common basis found in the literature), the heat transfer enhancement of the nanofluid is substantial and is in the range of 50–60% over water.

6.3. Alternative heat transfer enhancement comparison

As discussed by Pak and Cho [8], comparing heat transfer of a nanofluid to that of its base fluid at constant Reynolds number is generally not the best basis. Since the viscosity of a nanofluid is larger than its base fluid, a higher velocity for the nanofluid would be required to achieve the same Reynolds number. Alternatively, a constant velocity comparison was proposed [8] where it was found that, with an Al_2O_3/water nanofluid, the heat transfer coefficient of the nanofluid was 12% below that of the base fluid water. Such a comparison is made in Fig. 5 for the SiC/water nanofluid of this study. The results show that, at a constant velocity, the heat transfer coefficient of the SiC/water nanofluid is 7% below that of the base fluid water. This trend of lower heat transfer coefficients in nanofluids than in the base fluid also occurred in aluminum oxide/water, titanium oxide/water, and zirconium oxide/water nanofluids [8,9]. By using a constant velocity comparison, this reduced heat transfer coefficient of the nanofluids compared to

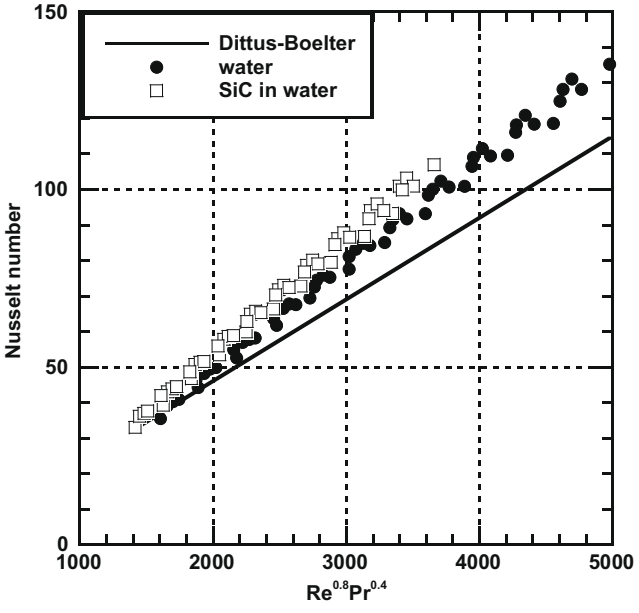

Fig. 3. Nusselt number comparison for SiC/water nanofluid.

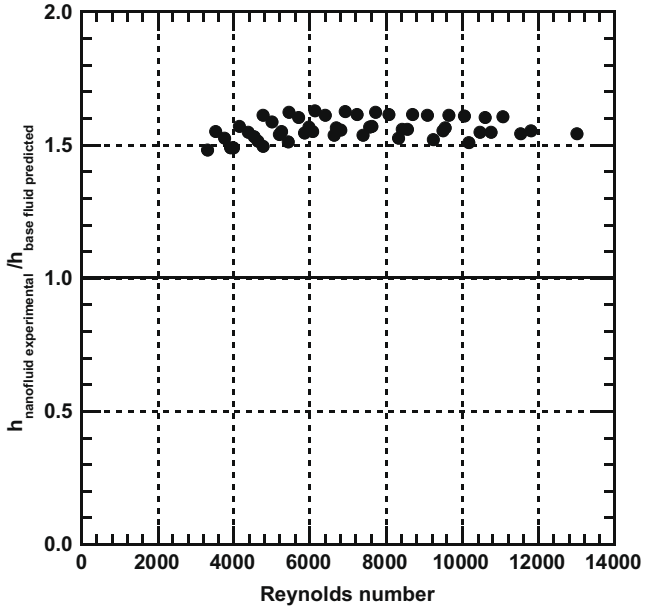

Fig. 4. Heat transfer enhancement of SiC/water nanofluid.

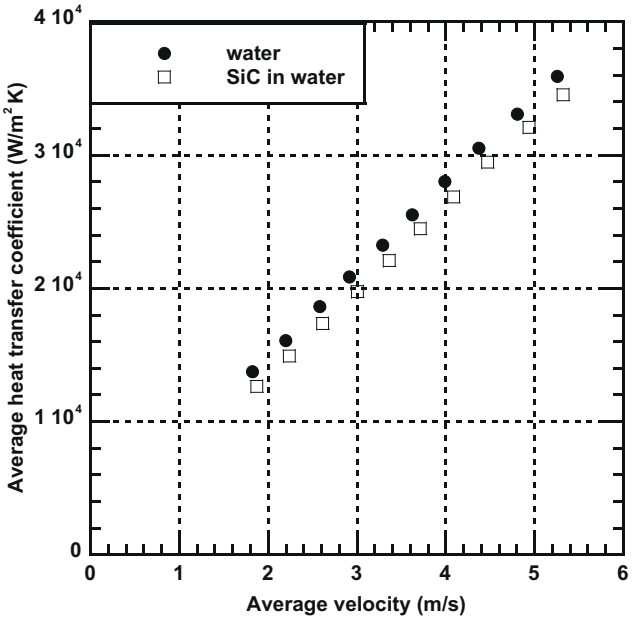

Fig. 5. Heat transfer coefficient of SiC/water nanofluid at constant velocity.

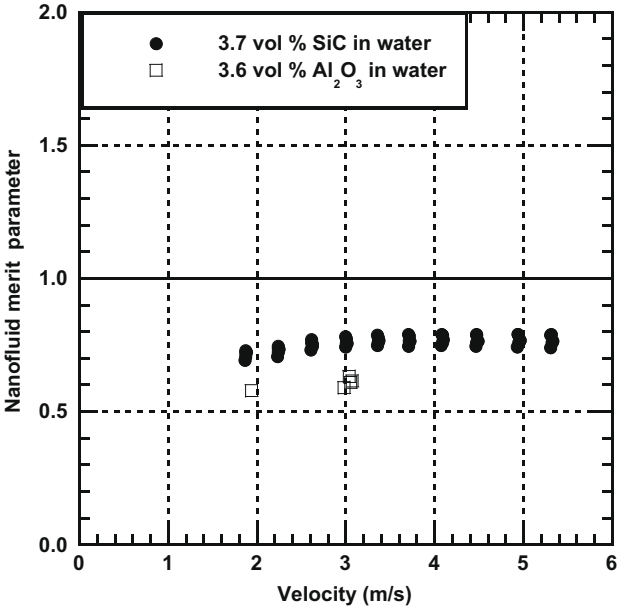

Fig. 6. Merit parameter comparisons for nanofluids.

that of the base fluid water occurs even though the thermal conductivity of the nanofluids is higher than that of the base fluid water in all cases. The reasons for this result are complex including the combination of thermal conductivity enhancement and viscosity increase found in the nanofluids. Enhanced thermal conductivity reduces resistance to thermal diffusion in the laminar sublayer of the boundary layer. However, increased viscosity increases the thickness of the sublayer and in turn increases its resistance to heat transfer. The net effect depends on the magnitudes of these competing phenomena, and the results for the SiC/water nanofluid are among the best of this group.

The potential of the SiC/water nanofluid is also seen in the Mouromtseff number Mo [15] that includes all of the fluid properties related by the Dittus–Boelter equation [14]

$$Mo = \frac{k^{0.6}\rho^{0.8}C_p^{0.4}}{\mu^{0.4}} \tag{6}$$

If both the base fluid and nanofluid heat transfer coefficients are reasonably predictable by a standard single-phase heat transfer correlation such as the Dittus–Boelter equation, then the Mouromtseff number can be used to indicate the heat transfer coefficient of the nanofluid compared to its base fluid under conditions of constant velocity by using the above equation. While the ratio of the Mouromtseff number for Al_2O_3/water nanofluid [8] to that for its base fluid water was 0.75, it was 0.89 for the SiC/water nanofluid of this study. Higher values are an indication of better heat transfer.

6.4. Nanofluid merit parameter

The concept of pumping power penalty is often used as a measure of comparison in augmented heat transfer situations, and some applications are more sensitive to it than others. In this study, the pumping power was combined with the heat transfer enhancement to produce a parameter indicative of the overall merit of a nanofluid. This nanofluid merit parameter is the ratio of the heat transfer enhancement to the pumping power increase, i.e. $(h_{nanofluid}/h_{base\ fluid})/(Power_{nanofluid}/Power_{base\ fluid})$. This parameter was calculated on the basis of constant flow velocities for the SiC/water nanofluids and its base fluid water flowing in smooth tubes. Results are shown in Fig. 6 for the SiC/water nanofluid of this study and an Al_2O_3/water nanofluid at a similar particle concentration [9]. The merit parameter is of the order of 0.8 for the SiC/water nanofluid while it is approximately 0.6 for the Al_2O_3/water nanofluid. A higher parameter value indicates more of a gain in the heat transfer enhancement compared to the pumping power penalty.

6.5. Nanofluid pressure drop

The pressure drop experimentally measured for both the SiC/water nanofluid and its base fluid water in this study were within 10% of theoretical values using their properties and friction factors obtained from the Moody diagram. This result is similar to those observed in other nanofluid studies [7–9].

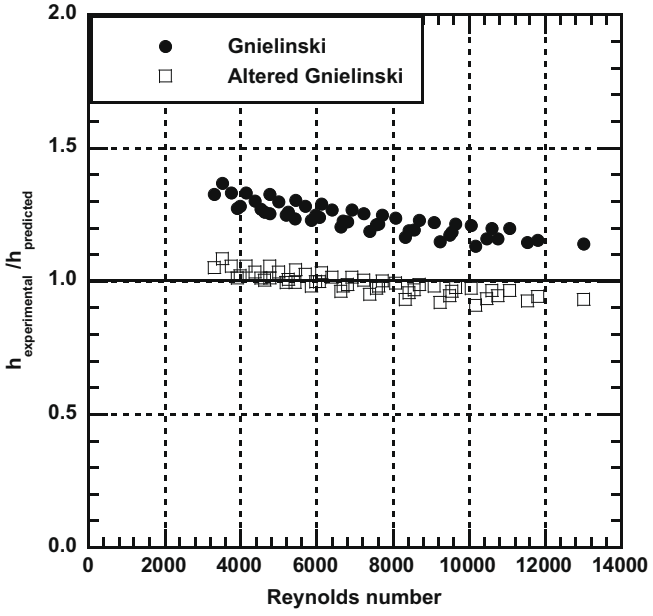

Fig. 7. Heat transfer enhancement of SiC/water nanofluid above prediction.

6.6. Nanofluid heat transfer prediction by liquid correlation

In Fig. 7, the nanofluid heat transfer data of Fig. 3 were compared to the predictions of the Gneilinski equation for the nanofluid. Here the predictions are from a standard single-phase turbulent heat transfer correlation based on the fluid being a pure liquid with the thermal and transport properties of the nanofluid. As seen in Fig. 7, the nanofluid heat transfer coefficient exceeded predictions in all cases ranging from 14% to 32% above the predictions.

The results of Fig. 7 are consistent with the Cu/water nanofluid data [10] and the Al_2O_3/water nanofluid data [8]. This enhancement over predictions points to a heat transfer mechanism beyond that of a pure liquid because of particle interactions.

In the work of Pak and Cho [8] and in a recent study [16], different Prandtl number dependencies were presented for nanofluids compared to pure liquids. A modified form of the Dittus–Boelter equation with a Prandtl number exponent of 0.5 was proposed [8], and an altered form of the Gneilinski equation was suggested [16]. The altered Gneilinski equation is seen in Fig. 7 to predict the SiC/water data well.

Only two slip mechanisms, Brownian diffusion and thermophoresis, were considered large enough to be responsible for measured nanofluid heat transfer enhancement over pure liquids [16]. These mechanisms cause the concentration of nanoparticles near the heat transfer surface to be different when the fluid is being heated or cooled. The postulated results are that nanofluid heat transfer rates over base fluids would increase when being heated and decrease when being cooled. In all the cases discussed previously, heat transfer rates were measured when the nanofluids were being heated, and nanofluid heat transfer coefficients were above their base fluids. In order to investigate the cooling condition, a series of experiments was performed in the present study using the cooling heat exchanger in the experimental facility. Here the average value of heat transfer coefficient was obtained from a logarithmic mean temperature difference calculation using the flow rates and the inlet and outlet temperatures of both the nanofluid and coolant.

Heat transfer results are shown in Fig. 8 for Nusselt numbers determined from measurements taken in the test section (fluid being heated) and in the cooler (fluid being cooled). The water data are well predicted by the Gneilinski equation independent of the source, i.e., test section or cooler, which validates the experimental approach used. The SiC/water nanofluid data were previously shown to be above prediction when being heated, which is consistent with the postulation [16]. These test section results are reproduced in Fig. 8. The SiC/water data from the cooler would be expected [16] to fall below predictions in Fig. 8, but the opposite is the case. Experimental Nusselt numbers are seen in Fig. 8 to lie along the same curve that is above predictions of the Gneilinski equation whether in heating or in cooling mode. These results do not support the mechanisms of Brownian diffusion and thermophoresis as being responsible for the enhanced SiC/water nanofluid heat transfer rates over the base fluid water.

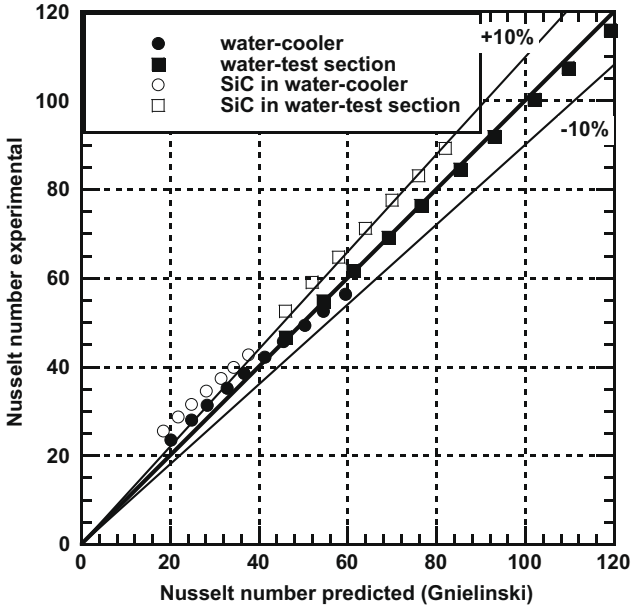

Fig. 8. Nusselt number for cooled and heated tests.

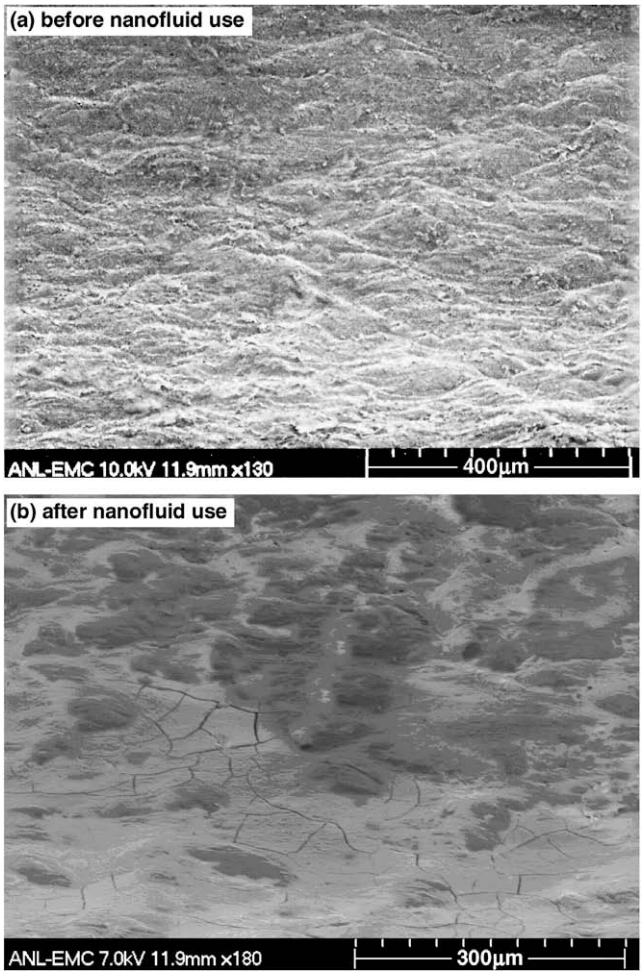

Fig. 9. SiC coating of test section tube surface.

Whether or not nanofluid heat transfer data are predicted by liquid correlations gives insight into the heat transfer mechanisms involved. Although the results shown in Fig. 8 do not support the mechanisms postulated [16], the prediction of nanofluid heat transfer using increased Prandtl number dependence is clear from Fig. 7. Predictability by liquid heat transfer correlations is not a key factor in assessing the potential of heat transfer enhancement associated with nanofluids. One nanofluid may show higher heat transfer enhancement than another even though both are predictable by liquid correlations. However, it is a positive result in terms of heat transfer enhancement when nanofluid heat transfer exceeds the predictions of liquid correlations. Such is the case with the SiC/water nanofluid.

6.7. Additional heat transfer mechanism

As discussed, heat transfer enhancement in various nanofluids has been attributed to different mechanisms. Recently, there have been additional discussions about particle coatings on heat transfer surfaces as being important [17]. No particle coating was detected with the Al_2O_3/water nanofluid [9], but, in a related study [17], it was concluded to be the source of the heat transfer enhancement. The SiC/water nanofluid of the present study was found to coat the test section surface. The stainless steel test section surface is shown in Fig. 9 before and after testing with the SiC/water nanofluid. It is evident that the nanoparticles, deposited in the low areas of the surface, formed a coating of the order of 100 particles thick. However, in this study the coating did not contribute to the heat transfer results as evidenced by water data that were unchanged before and after the SiC coating was formed. Also, no change in heat transfer rate over time was detected from the initial introduction of the SiC/water nanofluid into the facility.

7. Conclusions

The heat transfer rates were measured in the turbulent flow of a potential commercially viable nanofluid consisting of a 3.7% volume of 170-nm silicon carbide particles suspended in water. The properties and characteristics are favorable [11], and the fluid is available in large quantities. Heat transfer coefficient increase of 50–60% above the base fluid water was obtained when compared on the basis of constant Reynolds number. This enhancement is 14–32% higher than predicted by a standard single-phase turbulent heat transfer correlation pointing to heat transfer mechanisms that involve particle interactions. The data were well predicted by a correlation modified for Prandtl number dependence although experiments in the present study did not support the postulated mechanisms of Brownian diffusion and thermophoresis [16]. This increase in heat transfer rate over prediction is a favorable result for nanofluid heat transfer enhancement.

The pumping power penalty of the SiC/water nanofluid was shown to be less than that of an Al_2O_3/water nanofluid of comparable particle concentration. The two nanofluids were compared using a figure of the merit consisting of the ratio of heat transfer enhancement to pumping power increase. The merit parameter was 0.8 for the SiC/water nanofluid compared to 0.6 for the Al_2O_3/water nanofluid, which is favorable to the SiC/water nanofluid for applications that are pumping power sensitive.

Heat transfer rates on the basis of constant velocity showed 7% lower results for the SiC/water nanofluid than its base fluid water. However, these results are above those reported for Al_2O_3/water nanofluids with comparable particle concentrations. This result points to the direction of continued research in the development of a fully viable water-based nanofluid for commercial applications.

Acknowledgements

This work was sponsored by Michelin American Research and Development Corporation and by the U.S. Department of Energy, under Contract No. E-AC02-06CH11357 at Argonne National Laboratory, managed by the University of Chicago Argonne LLC (USA). Authors are grateful to Saint Gobain for providing the SiC/water nanofluid for this study.

References

[1] S.U.S. Choi, Z.G. Zhang, P. Keblinski, Nanofluids, in: H.S. Nalwa (Ed.), Encyclopedia of Nanoscience and Nanotechnology, vol. 6, American Scientific Publishers, Los Angles, CA, USA, 2004, pp. 737–757.
[2] J.A. Eastman, S.R. Phillpot, S.U.S. Choi, P. Keblinski, Thermal transport in nanofluids, Annu. Rev. Mater. Res. 34 (2004) 219–246.
[3] P. Keblinski, J.A. Eastman, D.G. Cahill, Nanofluids for thermal transport, Mater. Today (2005) 36–44.
[4] S.K. Das, S.U.S. Choi, H.E. Patel, Heat transfer in nanofluids – a review, Heat Transfer Eng. 27 (10) (2006) 3–19.
[5] S.K. Das, Nanofluids – the cooling medium of the future, Heat Transfer Eng. 27 (10) (2006) 1–2.
[6] S.K. Das, S.U.S. Choi, W. Yu, T. Pradeep, Nanofluids – Science and Technology, John Wiley & Sons Inc., Hoboken, New Jersey, USA, 2008.
[7] W. Yu, D.M. France, S.U.S. Choi, J.L. Routbort, Review and comparison of nanofluid thermal conductivity and heat transfer enhancements, Heat Transfer Eng. 29 (5) (2008) 432–460.
[8] B.C. Pak, Y.I. Cho, Hydrodynamic and heat transfer study of dispersed fluids with submicron metallic oxide particles, Exp. Heat Transfer 11 (1998) 151–170.
[9] W. Williams, J. Buongiorno, L.-W. Hu, Experimental investigation of convective heat transfer and pressure loss of alumina/water and zirconia/water nanoparticle colloids (nanofluids) in horizontal tubes, Trans. ASME J. Heat Transfer 130 (2008). pp. 7 (paper number 042412).
[10] Y. Xuan, Q. Li, Investigation on convective heat transfer and flow features on nanofluids, Trans. ASME J. Heat Transfer 125 (2003) 151–155.
[11] D. Singh, E. Timofeeva, W. Yu, J. Routbort, D. France, D. Smith, J.M. Lopez-Cepero, An investigation of silicon carbide–water nanofluid for heat transfer applications, J. Appl. Phys. 105 (2009). pp.7 (paper number 064306).
[12] R.J. Moffat, Describing the uncertainties in experimental results, Exp. Thermal Fluid Sci. 1 (1988) 3–17.
[13] V. Gneilinski, New equations for heat and mass transfer in turbulent pipe and channel flow, Int. Chem. Eng. 16 (2) (1976) 359–368.
[14] F.W. Dittus, L.M.K. Boelter, Heat transfer in automobile radiators of the tubular type, Univ. Calif. Publ. Eng. 2 (1930) 443–461.
[15] I.E. Mouromtseff, Water and forced-air cooling in vacuum tubes, Proc. IRE 30 (1942) 195–205.
[16] J. Buongiorno, Convective transport in nanofluids, Trans. ASME J. Heat Transfer 128 (2006) 240–250.
[17] S.J. Kim, I.C. Bang, J. Buongiorno, L.W. Hu, Surface wettability change during pool boiling of nanofluids and its effect on critical heat flux, Int. J. Heat Mass Transfer 50 (2007) 4105–4116.